

Multiple Accelerometers and Magnetometers Joint Calibration and Alignment

Konstantinos Papafotis*^{ID} and Paul P. Sotiriadis**^{ID}

Department of Electrical and Computer Engineering, National Technical University of Athens, 15780, Athens, Greece

*Student Member, IEEE

**Senior Member, IEEE

Manuscript received January 20, 2020; accepted February 5, 2020. Date of publication February 17, 2020; date of current version March 5, 2020.

Abstract—In this article, we introduce a computationally efficient algorithm for simultaneous joint calibration and axes alignment of multiple three-axis accelerometers or magnetometers. The proposed algorithm applies to ensembles of sensors of the same type, fixed to the same rigid platform. It compensates for all linear time-invariant distortions, such as scale factor, cross coupling, and offset, including the soft-iron and hard-iron distortions of the magnetometer. It can be implemented in a simple 12-step sequence and provides fast and accurate calibration without requiring any special piece of equipment.

Index Terms—Sensor systems, accelerometer, axes alignment, calibration, inertial sensors, magnetometer.

I. INTRODUCTION

Inertial and magnetic sensors are widely used in a broad variety of applications, from low-cost commercial systems (smartphones, activity trackers, etc.) to high-end marine, aerospace, and military ones. Typical application fields include navigation [1], attitude estimation [2], image stabilization [3], etc. Expensive, calibrated, high-accuracy sensors are used in many industrial and military applications. However, in commercial systems where cost is of ultimate importance, integrated, minimum-cost inertial, and magnetic sensors are preferred.

Inertial sensors in microelectromechanical form have become very popular over the past decades as they combine very small size with very low cost. Their main drawback is their large error characteristics [4] that must be compensated if accuracy is needed. Integrated magnetic sensors also require calibration; even if their inherent accuracy is satisfactory, when embedded to a system, the so-called hard-iron and soft-iron distortions must be removed.

Hard-iron distortion is the additive magnetic field created by magnetic objects attached to the reference frame of the sensor. Soft-iron distortion is the alteration of the existing magnetic field caused by ferromagnetic materials attached to the sensor's frame. Both these distortions are usually caused by electronic components in the vicinity of the sensor or materials used in the sensor's enclosure.

Note that postproduction factory calibration requires using special calibration equipment and/or services, both of which dramatically raise the final cost of the sensors. Therefore, factory calibration is not typically an option for low-cost systems. Thus, when accuracy is important, a calibration procedure that can be applied without using any special piece of equipment is required.

As far as three-axis accelerometers are concerned, most authors exploit the constant magnitude of the gravity for calibration purposes. More specifically, the calibration parameters are derived by measuring the sensor's output when it is placed in several different still positions. The calibration problem is posed either as a minimization problem [5]–[8] or as an estimation one [9].

In a similar way, for three-axis magnetometer calibration, the magnetic field of the earth is most commonly used as a reference. Using

the fact that the magnitude of the measured magnetic field should be locally constant (away of magnetic disturbances), the calibration parameters are calculated by solving a minimization [8], [10]–[14] or an estimation [15] problem.

The similarity in the calibration approach of accelerometers and magnetometers, based on similar physical principles, allows developing and using a single algorithm to calibrate both of them.

While there are several efficient calibration algorithms for a single accelerometer or magnetometer, in many applications, multiple sensors of the same kind are used to improve the measurement's accuracy [16]. Renaudin *et al.* [17] use a platform containing multiple magnetometers for orientation estimation. Six accelerometers arranged on a cube are used in [18] for a gyroscope-free inertial navigation application. In such cases, even if the sensors are individually calibrated, an extra step to align their sensitivity axes is required. This by itself is not a trivial step and requires multiple measurements and rotation matrices calculation.

In this article, we expand the algorithm introduced for a single-sensor's calibration in [8] to the case of multiple sensors. The proposed algorithm simultaneously addresses the calibration of multiple sensors and the alignment of their axes. It is based on a low computational cost iteration of a least-squares problem providing fast convergence and accurate calibration. It is applied using a simple 12-step sequence of platform's orientations and requires no special piece of equipment. Simulation and experimental results prove the algorithm's performance and efficiency.

II. SENSORS' MEASUREMENT MODEL AND THE PROBLEM OF CALIBRATION

In this section, we introduce the problem of simultaneous joint calibration and axes alignment of multiple three-axis accelerometers or magnetometers. To do so, we first derive a general model relating the sensors' measurements with the true values of the specific force or the magnetic field.

A. Accelerometer's Measurement Model

The measurement of an accelerometer is modeled as in [4] and [19],

$$y_a = f + T_{sf}f + T_{cc}f + h_a + \varepsilon \quad (1)$$

Corresponding author: Konstantinos Papafotis (e-mail: k.papafotis@gmail.com).
Associate Editor: G. Langfelder.
Digital Object Identifier 10.1109/LSSENS.2020.2974090

where y_a is the 3×1 measurement vector, f is the 3×1 true specific force vector, T_{sf} is the 3×3 diagonal matrix representing the scale-factor error, T_{cc} is the 3×3 matrix representing the cross-coupling error, h_a is the 3×1 accelerometer's offset vector, and ε represents the 3×1 random noise vector.

Defining matrix $T_a \triangleq I_3 + T_{sf} + T_{cc}$, where I_3 is the 3×3 identity matrix, (1) can be written as

$$y_a = T_a f + h_a + \varepsilon. \quad (2)$$

B. Magnetometer's Measurement Model

The measurement of a magnetometer is modeled following [11], [14], [20], and [21]

$$y_m = T_{sf} T_{cc} (T_{si} m + h_{hi}) + h_b + \varepsilon \quad (3)$$

where y_m is the 3×1 measurement vector, m is the 3×1 true magnetic field vector, T_{sf} denotes the 3×3 diagonal matrix representing the scale-factor error, T_{cc} is the 3×3 matrix representing the cross-coupling error, T_{si} is the 3×3 matrix modeling the soft-iron distortion, h_b is the 3×1 magnetometer's offset vector, h_{hi} is the 3×1 offset vector due to hard-iron distortion, and ε denotes the 3×1 random noise vector.

Defining matrices $T_m \triangleq T_{sf} T_{cc} T_{si}$ and $h_m \triangleq T_{sf} T_{cc} h_{si} + h_b$, the magnetometer's measurement model becomes

$$y_m = T_m m + h_m + \varepsilon. \quad (4)$$

C. Calibration as an Optimization Problem

The measurement models of the two sensors share the same form, and thus, we can use the general model of the following equation to formulate both sensors calibration process as the same optimization problem:

$$y = Tn + h + \varepsilon. \quad (5)$$

The purpose of the calibration is to estimate the 3×3 matrix T and the 3×1 vector h in order to minimize the measured noise ε strength.

The advantage of the proposed calibration method is that no special calibration equipment is needed, e.g., turntable for the accelerometer or Gauss magnetic chamber and Maxwell coils setup for the magnetometer. This implies that the true specific force or the true magnetic field vectors are unknown.

Note, however, that the magnitude of the true specific force and that of the true magnetic field are fixed when the accelerometer is still and the magnetometer is in static and uniform magnetic field. Assuming that the calibration measurements were taken under these conditions, without loss of generality, we assume that in (5), it is always $\|n\| = 1$. All norms in this letter are two-norms unless it is indicated otherwise.

Assuming K measurements y_1, y_2, \dots, y_K and writing (5) as $y_k = Tn_k + h + \varepsilon_k$, we define the cost function J_1 , capturing the total error

$$J_1 = \sum_{k=1}^K \|\varepsilon_k\|^2 = \sum_{k=1}^K \|y_k - Tn_k - h\|^2 \quad (6)$$

and form the following optimization problem whose solution is the calibration pair T, h and the field vectors $n_k, k = 1, 2, \dots, K$:

$$\begin{aligned} & \underset{T, h, n_k}{\text{minimize}} && J_1 \\ & \text{subject to} && \|n_k\| = 1, \quad k = 1, 2, \dots, K. \end{aligned} \quad (7)$$

Note that when (7) is used for a single-sensor's calibration, the calibration matrix T is derived subject to orthogonal multiplication

uncertainty. Specifically, if we replace T with TQ and n with $Q^T n$, where $Q \in O(3)$, the resulting measurement y is unaltered. Thus, if multiple sensors are individually calibrated using (7), a misalignment between their sensitivity axes is expected.

To overcome this, we expand the single-sensor calibration algorithm (7) to (multiple) L -sensor calibration algorithm incorporating the alignment of the sensors' axes as well. Let $n_k, k = 1, 2, \dots, K$ be the k th unit field vector, simultaneously exciting all L sensors, and denote by $y_{\ell,k}$ and $\varepsilon_{\ell,k}$ the corresponding measurement and error of the ℓ th sensor $\ell = 1, 2, \dots, L$. Moreover, let T_ℓ and h_ℓ be the ℓ th sensor's calibration matrix and offset vector, respectively. We write (5) in the matrix form

$$Y = TN + H + E \quad (8)$$

where Y is the measurements matrix, E is the errors matrix

$$Y = \begin{bmatrix} y_{1,1} & y_{1,2} & \dots & y_{1,K} \\ y_{2,1} & y_{2,2} & \dots & y_{2,K} \\ \vdots & \vdots & \ddots & \vdots \\ y_{L,1} & y_{L,2} & \dots & y_{L,K} \end{bmatrix}, \quad E = \begin{bmatrix} \varepsilon_{1,1} & \varepsilon_{1,2} & \dots & \varepsilon_{1,K} \\ \varepsilon_{2,1} & \varepsilon_{2,2} & \dots & \varepsilon_{2,K} \\ \vdots & \vdots & \ddots & \vdots \\ \varepsilon_{L,1} & \varepsilon_{L,2} & \dots & \varepsilon_{L,K} \end{bmatrix}$$

T and H are the calibration matrices in block form

$$T = \begin{bmatrix} T_1^T & T_2^T & \dots & T_L^T \end{bmatrix}^T$$

$$H = \begin{bmatrix} h_1^T & h_2^T & \dots & h_L^T \end{bmatrix}^T \begin{bmatrix} 1 & 1 & \dots & 1 \end{bmatrix}$$

and N is the set of true specific force or magnetic field vectors, common to all sensors

$$N = \begin{bmatrix} n_1 & n_2 & \dots & n_K \end{bmatrix}$$

As in the case of a single sensor, the cost function capturing the total error is expressed as

$$J_L = \sum_{\ell=1}^L \sum_{k=1}^K \|\varepsilon_{\ell,k}\|^2 = \|E\|_F^2 = \text{tr}(E^T E) \quad (9)$$

where the subscript F denotes the Frobenius norm [22]. The corresponding optimization problem becomes

$$\begin{aligned} & \underset{T, H, N}{\text{minimize}} && J_L \\ & \text{subject to} && \|n_k\| = 1, \quad k = 1, 2, \dots, K. \end{aligned} \quad (10)$$

Note that in (10), the set of unit-magnitude vectors n_k is common for all sensors, resulting in the alignment of their axes.

III. PROPOSED ALGORITHM

A typical way to solve optimization problems like (10) is by using the gradient descent or the Newton–Raphson methods. However, both of these methods depend strongly on a good initial estimate of the unknowns in order to converge. Especially in the magnetometer's case, finding an initial estimate is not trivial due to the uncertainty of soft-iron and hard-iron distortions reflecting on more challenging structures of T and H . In this article, we propose a computationally efficient, least-squares-based, iterative algorithm for solving (10) and achieving joint calibration and axes alignment of multiple sensors.

Algorithm 1: Proposed Algorithm.

Step 1: Initialize $T_l = I_3$ and $h_l = 0_{3 \times 1}$, $l = 1, 2, \dots, L$
 Step 2: Calculate \tilde{N} using (11) and form N as in (12)
 Step 3: Formulate matrices X and G according to (13)
 Step 4: Calculate X using (14)
 Step 5: Extract T and H from X
 Step 6: Calculate J_1 , for every sensor according to (6)
 Step 7: Repeat steps 2–6 until J_1 is sufficiently small for every sensor

A. Algorithm Description

In order to solve (10), we form a two-step algorithm. In the first step, we use an estimation of the calibration matrices T and H in order to solve for matrix N . Then, using the new matrix N , we improve our estimation of T and H while forcing the magnitude of the true specific force or magnetic field to be equal to one.

Given a set of K measurements, every iteration begins by calculating N using the estimate of T and H from the previous one. Assuming T is of full rank, we solve (8) using the least-squares method [23]

$$\tilde{N} = (T^T T)^{-1} T^T (Y - H). \quad (11)$$

To ensure that the true specific force or the true magnetic field vectors n_k , $k = 1, 2, \dots, K$ are of unit norm, we form the new estimate of N using the column vectors \tilde{n}_k , $k = 1, 2, \dots, K$ of \tilde{N} as follows:

$$N = \begin{bmatrix} \frac{\tilde{n}_1}{\|\tilde{n}_1\|} & \frac{\tilde{n}_2}{\|\tilde{n}_2\|} & \dots & \frac{\tilde{n}_K}{\|\tilde{n}_K\|} \end{bmatrix}. \quad (12)$$

Using this estimate of N , we rewrite (8) as

$$Y = XG + E \quad (13)$$

where

$$X = \begin{bmatrix} T_1^T & T_2^T & \dots & T_L^T \\ h_1^T & h_2^T & \dots & h_L^T \end{bmatrix}^T, \quad G = \begin{bmatrix} N \\ 1_{1 \times K} \end{bmatrix}.$$

The updated T and H are derived by solving (13) for X in the least-squares sense. Assuming G is of full rank, we get

$$X = YG^T(GG^T)^{-1}. \quad (14)$$

The proposed algorithm is summarized in Algorithm 1. It is initiated using $T_1 = T_2 = \dots = T_L = I_3$ and $h_1 = h_2 = \dots = h_L = 0_{3 \times 1}$.

The convergence of the algorithm could be evaluated in every iteration by using the cost function J_L . However, J_L does not provide any information about the calibration of each individual sensor. Thus, we prefer to use the cost function J_1 , evaluated for every sensor, as a metric of convergence.

B. Measurements Acquisition Procedure

The proposed algorithm jointly calibrates and aligns the axes of multiple accelerometers or magnetometers when they are all mounted on the same rigid platform. To that purpose, we recommend the 12-step measurement acquisition procedure introduced in [8], also shown in Fig. 1. Note that the steps in Fig. 1 should not be confused with the steps of Algorithm 1.

The (X, Y, Z) coordinate system in Fig. 1 denotes the platform's body frame, whereas the $(\tilde{X}, \tilde{Y}, \tilde{Z})$ coordinate system denotes the inertial reference frame that is fixed. The respective $y_{\ell,k}$, $\ell = 1, 2, \dots, L$, $k = 1, 2, \dots, 12$ is measured while the platform is still in each orientation.

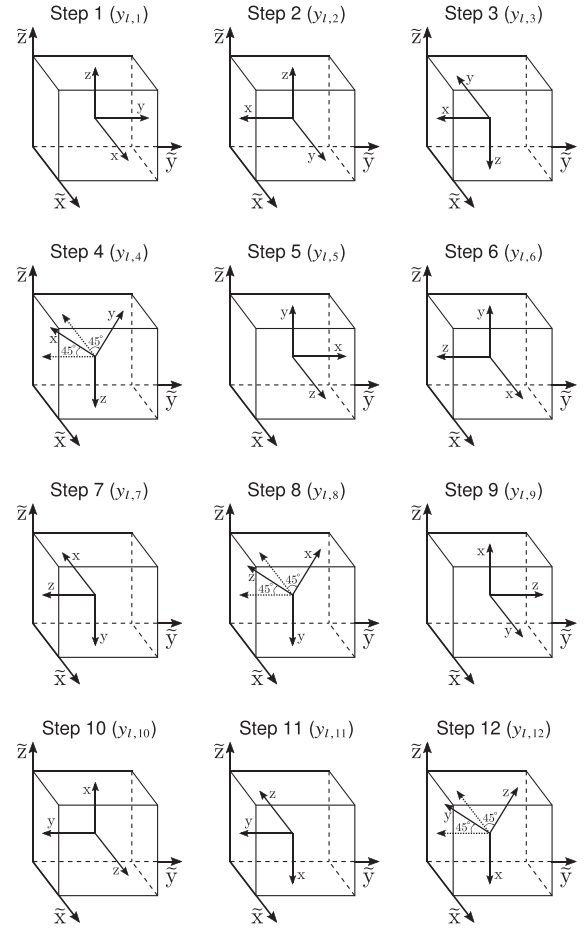


Fig. 1. Recommended sequence of approximate orientations.

Note that the orientations of the sensors' platform in Fig. 1 are meant to be approximate; no accuracy is needed. Orientation and placement of the sensor can be done by hand with an accuracy of about $\pm 15^\circ$ of Euler angle.

IV. EXPERIMENTAL AND SIMULATION RESULTS

The proposed algorithm's performance is evaluated using both sensors' measurements, from two three-axis magnetometers mounted on the same rigid platform, and simulated data of a large number of sensors ($L = 12$). Both measured and simulated data follow the measurement procedure in Fig. 1.

In Figs. 2 and 3, the algorithm's convergence using measured and simulated data, respectively, is presented. In both cases, the algorithm converges to a small value of the cost function in a way that appears to be monotonic.

In Fig. 2, the fractional mean magnitude error as a function of the iteration is also shown as a metric of the algorithm's accuracy. Note that it becomes significantly small after a few iterations, even before the cost function converges. This fact, in combination with the small computational burden of each iteration, demonstrates the computational efficiency of the proposed algorithm.

In Fig. 4, the raw and calibrated magnetometers' measurements magnitude, while the measurement platform is rotated in five different orientations, are presented. As the measurement took place away from any magnetic disturbance, the measured magnetic field should be of constant magnitude. As seen in Fig. 4, the magnitude of the raw

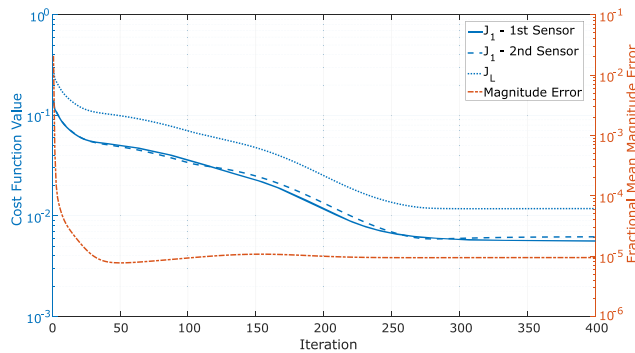


Fig. 2. Algorithm's convergence using measured data—Fractional mean magnitude error.

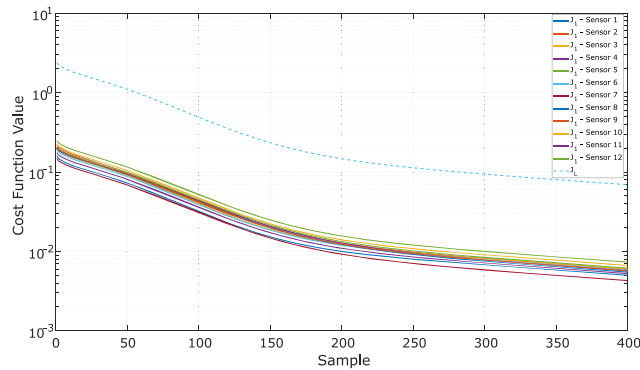


Fig. 3. Algorithm's convergence using simulated data.

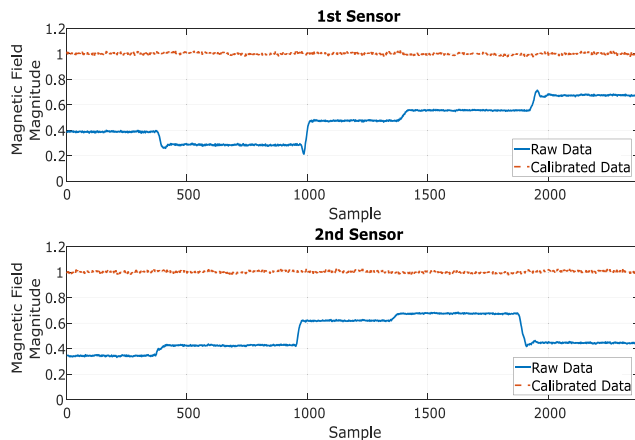


Fig. 4. Raw and calibrated magnetometer's measurements magnitude while the two sensors are placed in 5 different orientations.

measurements changes when the sensor is rotated while the magnitude of the calibrated data is constant and independent of the platform's orientation.

V. CONCLUSION

In this article, we introduced a computationally efficient algorithm for joint calibration and axes alignment of multiple three-axis accelerometers or magnetometers. It provides fast convergence and accurate calibration and axes alignment without requiring any special piece of equipment. The efficiency and the accuracy of the algorithm are demonstrated using both measured and simulated sensors' data.

ACKNOWLEDGMENT

This work was supported in part by Greece and the European Union (European Social Fund-ESF) through the Operational Program "Human Resources Development, Education and Lifelong Learning" in the context of the project "Strengthening Human Resources Research Potential via Doctorate Research" (MIS-5000432), implemented by the State Scholarships Foundation (IKY).

REFERENCES

- [1] C. Fischer, P. T. Sukumar, and M. Hazas, "Tutorial: Implementing a pedestrian tracker using inertial sensors," *IEEE Pervasive Comput.*, vol. 12, no. 2, pp. 17–27, Apr.–Jun. 2013.
- [2] S. O. H. Madgwick, A. J. L. Harrison, and R. Vaidyanathan, "Estimation of IMU and MARG orientation using a gradient descent algorithm," in *Proc. IEEE Int. Conf. Rehabil. Robot.*, Jun. 2011, pp. 1–7.
- [3] C. Chu, "Video stabilization for stereoscopic 3D on 3D mobile devices," in *Proc. IEEE Int. Conf. Multimedia Expo.*, Jul. 2014, pp. 1–6.
- [4] P. D. Groves, *Principles of GNSS, Inertial, and Multisensor Integrated Navigation Systems*. Norwood, MA, USA: Artech House, 2013.
- [5] X. Lu, Z. Liu, and J. He, "Maximum likelihood approach for low-cost MEMS triaxial accelerometer calibration," in *Proc. 8th Int. Conf. Intell. Human–Mach. Syst. Cybern.*, Aug. 2016, vol. 1, pp. 179–182.
- [6] N. Ammann, A. Derksen, and C. Heck, "A novel magnetometer-accelerometer calibration based on a least squares approach," in *Proc. Int. Conf. Unmanned Aircr. Syst.*, Jun. 2015, pp. 577–585.
- [7] I. Frosio, F. Pedersini, and N. A. Borghese, "Autocalibration of MEMS accelerometers," *IEEE Trans. Instrum. Meas.*, vol. 58, no. 6, pp. 2034–2041, Jun. 2009.
- [8] K. Papafotis and P. P. Sotiriadis, "MAG.I.C.AL—A unified methodology for magnetic and inertial sensors calibration and alignment," *IEEE Sensors J.*, vol. 19, no. 18, pp. 8241–8251, Sep. 2019.
- [9] M. Glueck, A. Buhmann, and Y. Manoli, "Autocalibration of MEMS accelerometers," in *Proc. IEEE Int. Instrum. Meas. Technol. Conf.*, May 2012, pp. 1788–1793.
- [10] R. Alonso and M. D. Shuster, "TWOSTEP: A fast robust algorithm for attitude-independent magnetometer-bias determination," *J. Astronaut. Sci.*, vol. 50, pp. 433–451, 2002.
- [11] Y. Wu and W. Shi, "On calibration of three-axis magnetometer," *IEEE Sensors J.*, vol. 15, no. 11, pp. 6424–6431, Nov. 2015.
- [12] M. Kok and T. B. Schön, "Maximum likelihood calibration of a magnetometer using inertial sensors," *IFAC Proc.*, vol. 47, no. 3, pp. 92–97, 2014.
- [13] M. Kok and T. B. Schön, "Magnetometer calibration using inertial sensors," *IEEE Sensors J.*, vol. 16, no. 14, pp. 5679–5689, Jul. 2016.
- [14] J. F. Vasconcelos, G. Elkaim, C. Silvestre, P. Oliveira, and B. Cardeira, "Geometric approach to strapdown magnetometer calibration in sensor frame," *IEEE Trans. Aerosp. Electron. Syst.*, vol. 47, no. 2, pp. 1293–1306, Apr. 2011.
- [15] Y. Wu, D. Zou, P. Liu, and W. Yu, "Dynamic magnetometer calibration and alignment to inertial sensors by Kalman filtering," *IEEE Trans. Control Syst. Technol.*, vol. 26, no. 2, pp. 716–723, Mar. 2018.
- [16] I. Skog, J. Nilsson, and P. Händel, "An open-source multi inertial measurement unit (MIMU) platform," in *Proc. Int. Symp. Inertial Sensors Syst.*, Feb. 2014, pp. 1–4.
- [17] V. Renaudin, M. H. Afzal, and G. Lachapelle, "New method for magnetometers based orientation estimation," in *Proc. IEEE/ION Position, Location, Navigation Symp.*, May 2010, pp. 348–356.
- [18] E. Akeila, Z. Salcic, and A. Swain, "Implementation, calibration and testing of GFINS models based on six-accelerometer cube," in *Proc. IEEE Region 10 Conf.*, Nov. 2008, pp. 1–6.
- [19] A. Noureldin, T. B. Karamat, and J. Georgy, *Fundamentals of Inertial Navigation, Satellite-Based Positioning and Their Integration*. Berlin, Germany: Springer-Verlag, 2013.
- [20] M. Kok, J. D. Hol, T. B. Schön, F. Gustafsson, and H. Luinge, "Calibration of a magnetometer in combination with inertial sensors," in *Proc. 15th Int. Conf. Inf. Fusion*, Jul. 2012, pp. 787–793.
- [21] J. Metge, R. Mégret, A. Giremus, Y. Berthoumieu, and T. Décamps, "Calibration of an inertial-magnetic measurement unit without external equipment, in the presence of dynamic magnetic disturbances," *Meas. Sci. Technol.*, vol. 25, no. 12, 2014, Art. no. 125106. [Online]. Available: <http://stacks.iop.org/0957-0233/25/i=12/a=125106>
- [22] R. A. Horn and C. R. Johnson, *Matrix Analysis*. Cambridge, U.K.: Cambridge Univ. Press, 2013.
- [23] G. Strang, *Linear Algebra and Its Applications*. Pacific Grove, CA, USA: Brooks/Cole, 2007.